Original article

Folia Neuropathologica

High resolution proton nuclear magnetic resonance (^{1}H NMR) spectroscopy of surviving C6 glioma cells after X-ray irradiation

Łukasz Matulewicz[1], Anna Cichoń[2], Maria Sokół[2], Waldemar Przybyszewski[3], Magdalena Głowala-Kosińska[4], Mirosław Gibas[5]

[1]Department of Radiotherapy and Brachytherapy Planning, Maria Skłodowska-Curie Memorial Cancer Center and Institute of Oncology, Gliwice, [2]Department of Medical Physics, Maria Skłodowska-Curie Memorial Cancer Center and Institute of Oncology, Gliwice, [3]Center for Translational Research and Molecular Biology of Cancer, Maria Skłodowska-Curie Memorial Cancer Center and Institute of Oncology, Gliwice, [4]Department of Bone Marrow Transplantation and Oncohematology, Maria Skłodowska-Curie Memorial Cancer Center and Institute of Oncology, Gliwice, [5]Department of Organic Chemistry, Bioorganic Chemistry and Biotechnology, Silesian University of Technology, Gliwice, Poland

Folia Neuropathol 2013; 51 (1): 33-43 DOI: 10.5114/fn.2013.34194

Abstract

Purpose: *To study biochemical response of living model of glioma to X-rays irradiation using high resolution proton nuclear magnetic resonance (^{1}H NMR) spectroscopy.*

Material and methods: *Rat glioma C6 cells were irradiated with 3.8 Gy (D_0, the 37% clonogenic survival dose) of X-rays from a teletherapy unit at the dose rate 8.8 Gy/min. After irradiation the cells were incubated at 37°C/5%CO_2/95%O_2 for various period of incubation (24, 48, 72 and 96 hours) in the fresh medium. The high resolution ^{1}H NMR spectra of the agarose-cell mixtures (2 x 10^7 cells/ml) were acquired using a Varian Inova-300 multinuclear pulsed NMR spectrometer operating at the ^{1}H resonance frequency of 300 MHz. The mean spectra were obtained as the averages of six independent measurements.*

Results: *The statistically significant increase in the CH2/CH3 lipid signals ratio in the C6 cells after irradiation with 3.8 Gy dose and incubation for 24-96 h was observed.*

Conclusions: *Our method of the sample preparation enables the metabolic effects of irradiation to be observed in viable cells, which can effectively support the identification of the spectroscopic changes in vivo. Application of the gel suspensions in the NMR studies has advantages over the usual liquid suspensions in terms of improved reproducibility of the data and cell viability, with no net loss of the spectral quality.*

Key words: *^{1}H NMR spectroscopy, C6 glioma, X-ray irradiation.*

Introduction

In many publications the appearance of mobile lipid (ML) signals in ^{1}H NMR spectra (mainly deriving from fatty acyl chains) have been associated with numerous cellular phenomena including cell proliferation or apoptosis [1,2,6,9,16,17,22,24,26,30,31,37,38,40,45,46,51]. Though radiation therapy is widely used in cancer therapy, only few works have been published on the

Communicating author:

Łukasz Matulewicz, PhD, Department of Radiotherapy and Brachytherapy Planning, Maria Skłodowska-Curie Memorial Cancer Center and Institute of Oncology, Gliwice Branch, Wybrzeże Armii Krajowej 15, 44-101 Gliwice, Poland, e-mail: lukasz.matulewicz@io.gliwice.pl

application of ^{1}H NMR to irradiated cells *in vitro* [13,14, 38,42-44].

The aim of this study was to investigate the biochemical response of living model of gliomato X-rays irradiation. This model reflected the intra-glioma cell compartment only, without modelling other neural tissue cells, extracellular space, vessels, cerebrospinal fluid etc. In the present study we examined the C6 rat glioma cell line. Its pathological and growth characteristics are similar to those observed in the case of human gliomas [28,36]. This cell line has been extensively studied radiobiologically [21,23,25,34,39] and using ^{1}H NMR [2,3,7,8,35] or ^{13}C NMR technique [10] but to the best of our knowledge it has never been studied after X-rays irradiation by means of ^{1}H NMR spectroscopy.

Material and methods

Cell cultures

The rat C6 glioma cell line was obtained from ATCC (American Type Culture Collection; CRL-2199). The cells were routinely maintained as a monolayer culture in Dulbecco's minimum essential medium (DMEM, Sigma), supplemented with 12% foetal bovine serum (FBS, Gibco) and antibiotic (80 µg/ml gentamicin, Polfa). The cells were incubated at 37°C/5%CO_2/95%O_2 in polystyrene flasks (Nunc Easy Flask 75 cm^2).

Irradiation and postradiation incubation

Irradiation was performed at room temperature with X-ray photons generated by a linear Clinac-600C/D accelerator (Varian). The vertical beam was projected to a 18 × 18 cm^2 field size (SSD [source surface sistance] = 80 cm). The C6 glioma cell cultures received a one-time dose of 3.8 Gy (D_0), 37% clonogenic survival dose [50] at a dose rate of 8.8 Gy/min. The control cells were not exposed. After irradiation the cells were incubated up to 24, 48, 72 or 96 hours in the fresh medium.

Before the NMR measurements, the cells were harvested by trypsinization. Only the cells actively adhering to the flask bottom were collected. Then the cells were centrifuged (at 112 RCF, 5 min.), washed twice with 0.9% NaCl solution (pH 7.4, phosphate-buffered saline) made with D_2O (Sigma-Aldrich) and counted using a Bürker chamber.

Metabolic activity

Metabolic activity of the cells was determined using MTS (3-(4,5-dimethylthiazol-2-yl)-5-(3-carboxymethoxyphenyl)-2-(4-sulfophenyl)-2H-tetrazolium) colorimetric assay (CellTiter 96® AQueous One Solution Cell Proliferation Assay, Promega Corp., Madison, WI, USA). The cells from different time points after irradiation and the non-irradiated cells were incubated for 2 hours in 96-well plates (16 wells for every time point) with DMEM without phenol red and MTS solution (volume ratio 5 : 1). BioTek ELX800 was used for measurements of formazan absorbance at light wave length of 490 nm. For each time point (irradiated and non-irradiated at 24 h, 48 h, 72 h, 96 h), six independent experiments were performed.

Determination of cell cycle phases

The distribution of the cell cycle population was analysed by a flow cytometry on a FACSCanto (BD, USA). The cells were fixed in 70% ethanol (–20°C) for 30 min, centrifuged and washed with PBS, treated with 100 µl/ml RNAse (Sigma-Aldrich) for 15 min at room temperature, stained with 100 µg/ml propidium iodide (Sigma-Aldrich) for 10 min and then analysed. For each time point (24 h, 48 h, 72 h, 96 h for both the irradiated and non-irradiated cells), six independent measurements were performed.

^{1}H NMR measurements

Agarose powder (Sigma, Type I) was dissolved in D_2O at 0.15% (w/w). 300 µl of agarose solution at 37°C was mixed with pellet of cells (2 × 10^7 cells). The agarose-cell mixture was transferred rapidly to a 5-mm NMR tube and placed in the spectrometer (20°C). Our own cells' inserting method was applied in which two layers of pure agarose in D_2O were separated by a layer containing the cells (as showed in Fig. 1). This method of application enables three-fold increase in the concentration of the cells keeping the loading requirement of the NMR measurement.

The high resolutionone-dimensional ^{1}H NMR spectra were acquired using a Varian Inova-300 multinuclear pulsed NMR spectrometer operating at the ^{1}H resonance frequency of 300 MHz (the parameters: pulse 45°, spectral window = 4000 Hz; single acquisition time = 3.744 s; d1 = 2 s, number of repetitions = 400). For each time point (control, 24 h, 48 h, 72 h, 96 h), six independent measurements were performed.

Despite the depletion of the nutrients in the NMR tube for the agarose-immobilized cells and the accumulation of the metabolic waste products, the short duration of the ^{1}H NMR measurement (less than 1 hour) enables keep-

ing the living cells in the sample without applying perfusion [27]. In the case of the perfused systems, the flow of medium adds to the difficulty in suppressing the water peak in the ^{1}H NMR spectra. The gas bubbled into the NMR tube and that produced due to the cells' metabolic processes generate gas bubbles which, in turn, decrease the magnetic field homogeneity and cause differences in the magnetic susceptibility between the gas and the liquid in the NMR-detected region of the sample. This broadens the resonances in the spectrum and therefore reduces spectral resolution [27].

The preparation of each sample and the subsequent NMR measurement in our experiment lasted for about 40 min. However, despite this short measurement time and since a perfusion system was not used, it was necessary to determine the stability of the NMR spectra of the embedded cells in agarose in time. No statistical differences in the signal intensities in the range of 1.18-1.43 were observed ($p > 0.9$, Kruskal-Wallis test) up to 3 hours after the embedding of the cells in the NMR tube.

Additionally, the spectra from the dead cells were acquired after two weeks after embedding the cells in the NMR tube. The marked increase of the lactate signal in these spectra, as compared to that in the living cells' ones, can be explained by the increased anaerobic metabolism.

Analysis of the spectra

The measured FID (free induction decay) signals were zero-filled to 32K points and Fourier transformed with apodization (1 Hz) to the frequency domain using MestReCv. 2.3 software (Mestrelab Research, Spain). The spectra were manually phase-corrected (zero and first order), referenced to the lactate doublet at 1.33 ppm (parts per million) and normalized to unit area within the range from 0 to 4.2 ppm. The CH_2/CH_3 parameter was calculated according to Eq. 1 (the ranges of the lipid bands were selected after Hiltunen *et al*. [18]):

$$\frac{CH_2}{CH_3} = \frac{\int_{1.18\ ppm}^{1.43\ ppm} f(x)dx}{\int_{0.73\ ppm}^{1.06\ ppm} f(x)dx} \quad \text{Eq. 1}$$

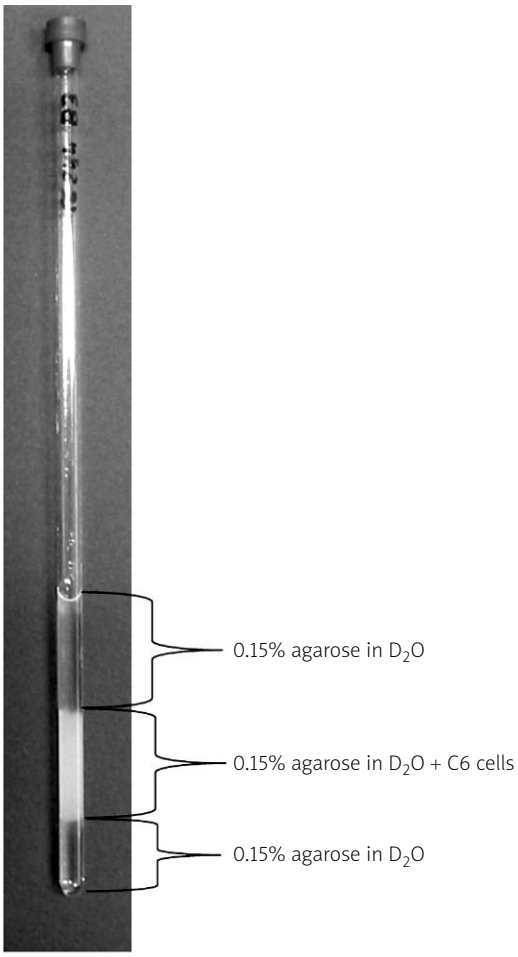

Fig. 1. Photograph of cells and agarose inserting 3-layers scheme inside the NMR tube.

This parameter has been proposed as a quantitative method for the estimation of a cell damage (often interpreted as an apoptotic death index) [6,12,15,29,32].

Table I. Cell viability measured by MTS assay for all time groups after irradiation

Time after irradiation	Relative metabolic activity (viability) of irradiated cells vs. non-irradiated cells at the same time point
24 h	85.62 ± 14.45*
48 h	86.20 ± 17.42
72 h	86.70 ± 16.67
96 h	88.19 ± 9.46

**Mean values from six independent experiments (% ± SEM)*

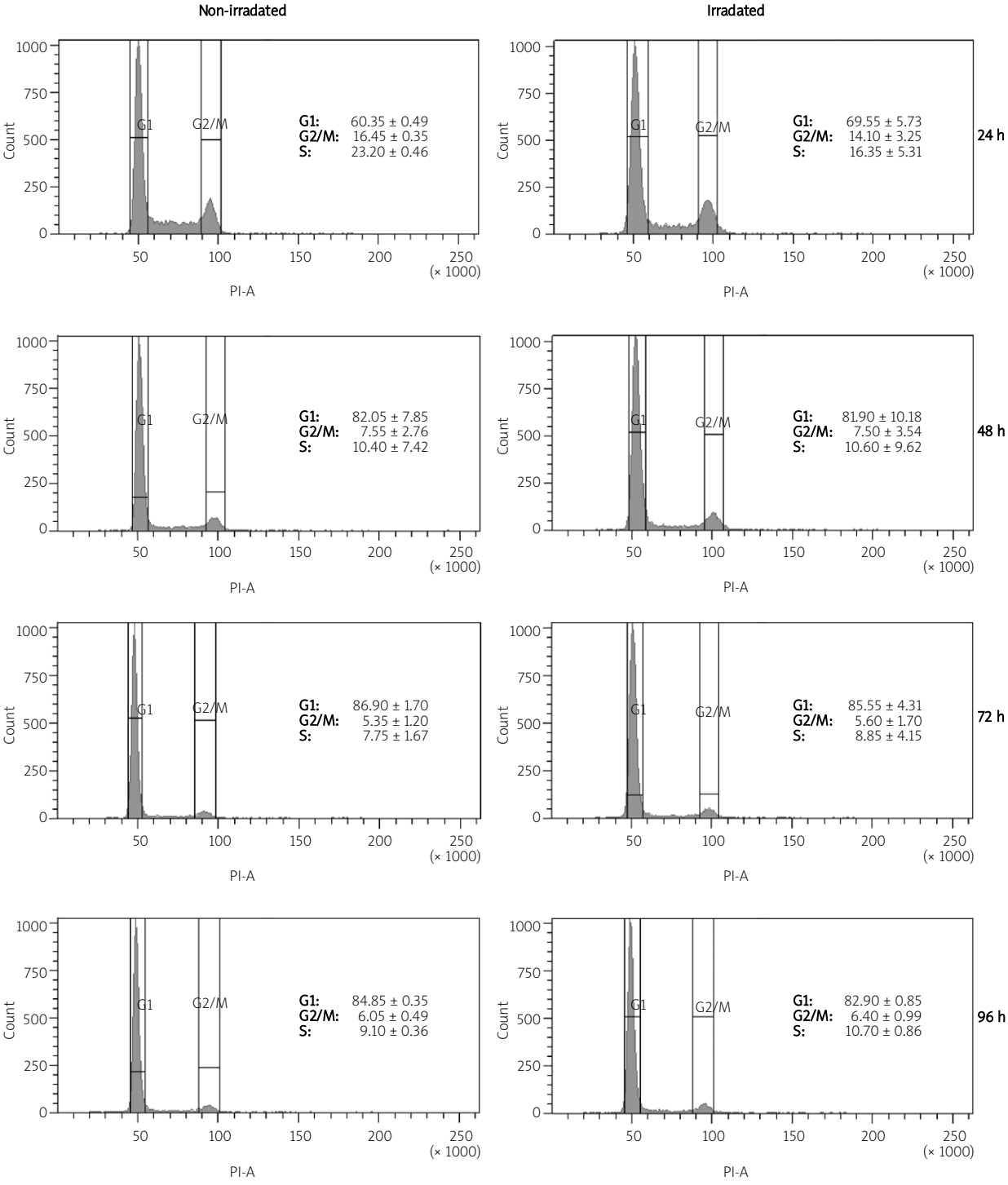

Fig. 2. Histograms picturing cytometric cell cycle analysis with cell count on vertical axis and DNA content on horizontal axis. Mean percentage values (± SD, standard deviation) of the cells arrested at the given G1, G2/M and S phases are presented.

To determine the contribution of the lactate doublet into the methylene lipid range of 1.18-1.43 ppm, the method proposed by Hiltunen *et al.* [18] for blood plasma was adopted. Taking into account the universality of the lipids in *Eucaryota*, the method can be applied also to the spectra analysis of the C6 cells.

It should be noted that within the selected CH_2 and CH_3 lipid ranges, apart from the lactate signal contribution, there is also a small contribution from isoleucine (1.0 ppm), leucine (1.0 ppm), valine (1.0 ppm), threonine (1.3 ppm) and fucose (FucI 1.3 ppm, FucII 1.2 ppm, FucIII 1.3 ppm) [41].

Results

Vitality of the cells

Mean values of the relative metabolic activity (cell viability) for all the time groups after irradiation received by the MTS method are presented in Table I. The statistically significant differences in the optical density at 490 nm (being directly proportional to the metabolic activity and the number of viable cells) between their radiated and non-irradiated cells at the different time points were observed as estimated by Mann-Whitney test (p = 0.000000). However, there was no statistical difference (p > 0.62) in the viability percentage between the irradiated cells incubated with a different period of time (24, 48, 72 and 96 h).

It is worth noting that only the cells actively adhering to the flask bottom were collected. This enabled a homogeneous surviving cell population to be measured, without any potential cell debris contamination.

Determination of cell cycle phases and hypodiploid DNA content

The results of the cytometric cell cycle analysis are shown in Fig. 2 graphically and also as the percentage values of the cells arrested at the given G1, G2/M and S (100% –G1, –G2/M) phases. The cells' percentages at the G1, G2/M and S stages are similar for both the irradiated cells and non-irradiated ones. The significant difference is observed only for the cells after 24 h of incubation. In this case the percentage of the mitotically inactive cells in G1 is higher, while the amount of the cells in the G2/M and S phases is decreased (both for the irradiated cells and non-irradiated ones). This suggests a slower proliferation frequency in the cell culture after 24 h of incubation for both the irradiated and non-irradiated cells. Presumably it is due to the increasing cell density during the exponential growth in the culture flask. For the irradiated cells the proliferation is expected to be additionally suppressed as compared to the non-irradiated ones which is reflected in the flow cytometry results (Fig. 2). However, the latter phenomenon is significant only for the incubation time of 24 h after irradiation.

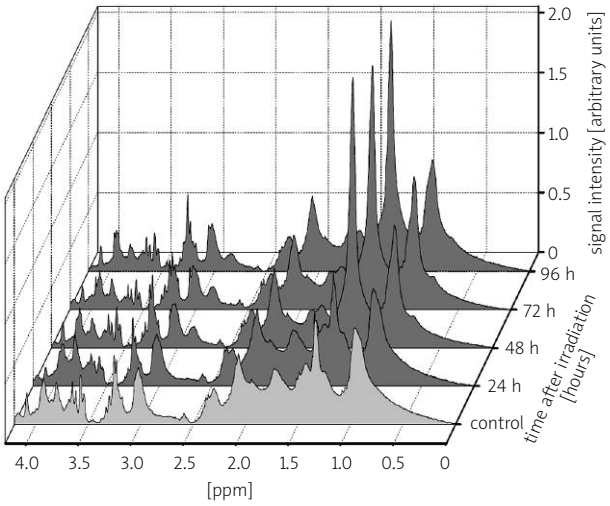

Fig. 3. Comparison of mean high-resolution 300 MHz ^{1}H NMR spectra in the range of 0-4.2 ppm from N = 6 independent measurements for the C6 cells after different time of postradiation incubation.

The amount of the cells in sub-G1 (the percentage of the hypodiploid DNA in a total DNA content) is below 1% of the total cells' amount for all the samples under study, which means the potential apoptotic percentage to be below the cytometry precision level [33]. This allows for excluding the apoptosis as the process markedly influencing the cells' population.

^{1}H NMR measurements results

Figure 3 compares the mean spectra from six independent measurements of the non-irradiated C6 cells (control) and those incubated 24-96 h after irradiation. The mean control spectrum (obtained from the non-irradiated cells) was subtracted from the mean spectra of the irradiated and incubated cells (24-96 h) and the resulting difference spectra are shown in Fig. 4. The intense peak at 1.32 ppm is observed in the difference spectra, deriving mainly from the methylene groups of the fatty acyl chains of lipids. Along with the increase in the CH_2 lipid band also a slight increase

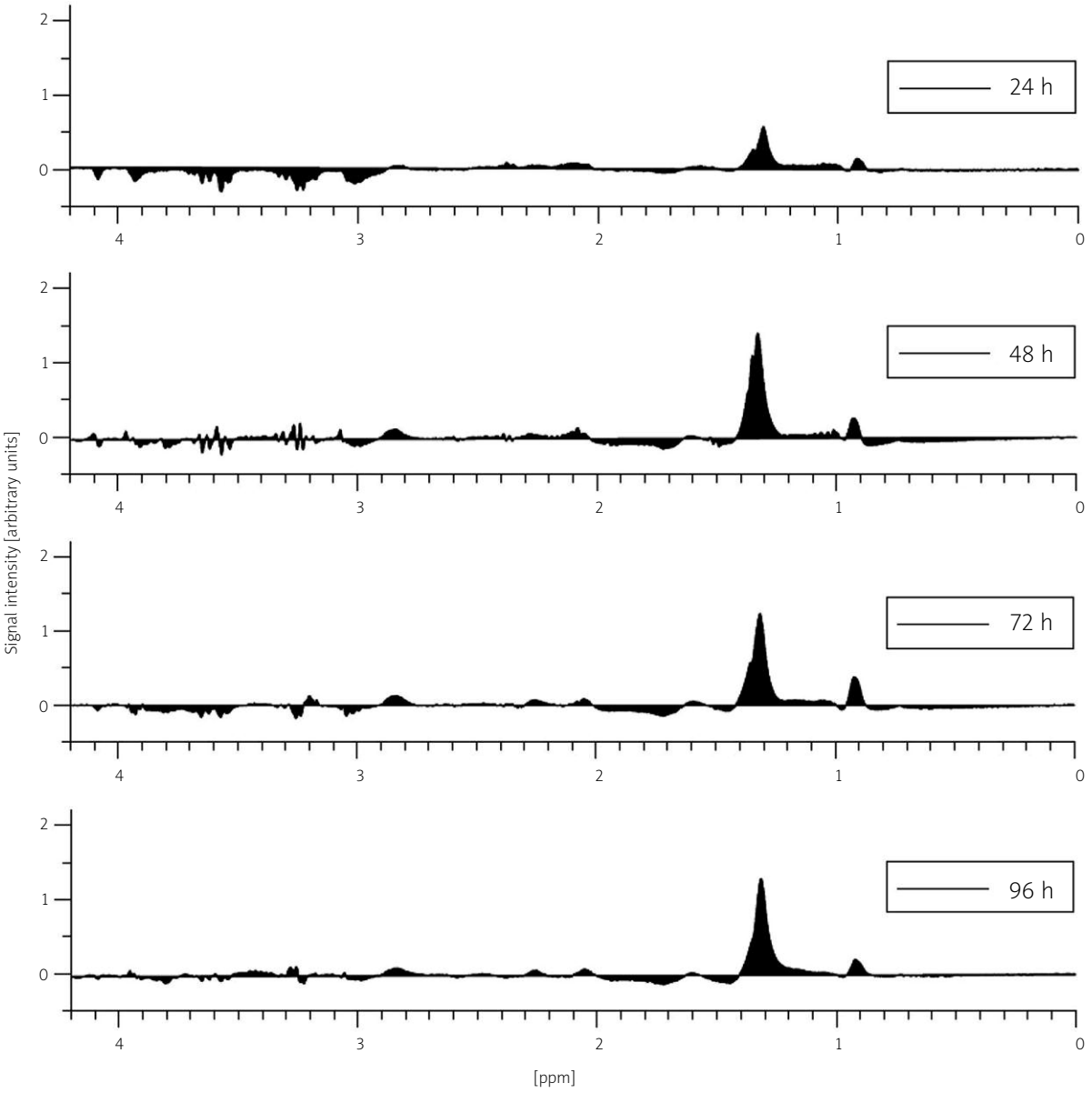

Fig. 4. The difference (irradiated – control) high-resolution 300 MHz ^{1}H NMR spectra in the range of 0-4.2 ppm from *N* = 6 independent measurements for the C6 cells after different time of postradiation incubation.

in the CH_3 lipid terminal groups signal at 0.92 ppm is observed on irradiation.

As seen in Fig. 5 the mean value of the CH_2/CH_3 lipid signals ratio increases in time after irradiation, contrary to that for the non-irradiated cells. All the mean values of the CH_2/CH_3 ratio calculated from the spectra of the irradiated cells differ significantly ($p < 0.01$, Mann-Whitney test) from the corresponding mean values obtained for the non-irradiated cells (control). At the incubation times above 48 h, a plateau is observed and the mean values of the CH_2/CH_3 ratio for the irradiated and incubated cells do not differ significantly ($p > 0.1$, Kruskal-Wallis test).

Lactate analysis

In order to estimate the lactate resonance area within the methylene lipid 1.18-1.43 ppm range, the methodology proposed by Hiltunen *et al.* for the lipid analysis of blood plasma [18] was adapted. Figure 6 shows the examples of the Lorentz functions fittings within

the range of 1.18-1.43 ppm for the non-irradiated cells, the irradiated and incubated ones as well as for the dead cells (acquired two weeks after the embedding in agarose, Fig. 6A).The Kruskal-Wallis test does not show statistically significant differences in the lactate resonance area in the spectra obtained from the non-irradiated cells, and the cells irradiated and incubated for 24 h, 48 h, 72 h and 96 h ($p > 0.4$). The mean value of the lactate doublet area equals 2.80% (± 0.27) for both the control and the irradiated samples, beings five-fold less than that got from the spectrum of the dead cells (15.57%) (Fig. 6A).

Discussion

In vitro studies on cells to date revealed that ionizing radiation may induce many effects like: metabolism changes [48], cell cycle delay [19], DNA damage [47], cell membrane damage [4] and, finally, apoptotic or necrotic death [49]. The present study reports the variation in the ^{1}H-NMR visible mobile lipids that occurred in C6 cells after the X-ray irradiation and incubation. Our experiment showed the CH_2/CH_3 lipids ratio to increase after irradiation with no evident later stage apoptosis indicating DNA damage as revealed by the flow cytometry. It should be stressed again that only the cells actively adhering to the flask bottom were measured at a particular moment after the irradiation to avoid the effects from the dead cells and the cellular debris. It is worth noting that the CH_2/CH_3 signal intensity ratio increase from 1.01 (control) to 1.35 (at 96 h) coincides well with the data published by Shih *et al.* [46]. In the mentioned work (for the MRC-5 cells after Hg exposure) the CH_2/CH_3 signal intensity ratio increase from 0.92 (control) to 1.31 (2-24 h) was reported. Shih *et al.* interpreted their results as being due to necrosis, whereas the variations of the 2.02 signal (at 24 h after Cd treatment) as being correlated with apoptosis (on the basis of the phosphatidylserine externalization measurements).

There are numerous ^{1}H-NMR *in vitro* publications reporting that the CH_2 and CH_3 mobile lipids are closely associated with the cell death processes [1,5,6,11,12, 20,30,31,45]. Also *in vivo* studies show that the ^{1}H-NMR visible mobile lipids correlate with apoptosis [17,24] or necrosis [22,51]. However, Santini *et al.* in one of their publications proved that the ^{1}H-NMR mobile lipids are not always associated with overt apoptosis [43]. The chromatin dye Hoechst 33258 and the DNA fragmentation assays showed no overt apoptosis up to 7 days

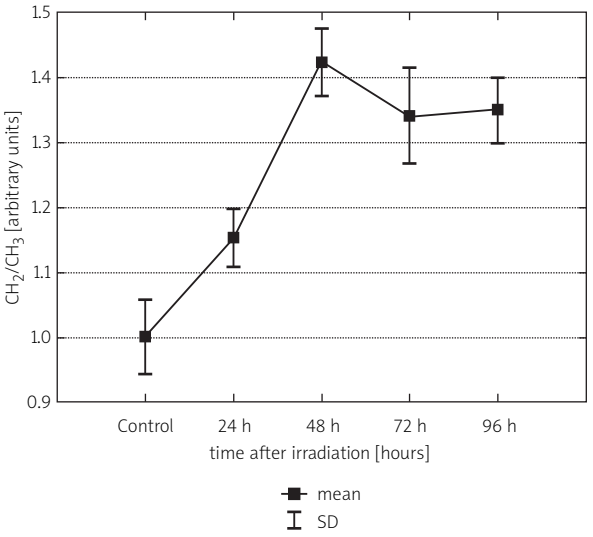

Fig. 5. Mean values of CH_2/CH_3 ratio after different time of postradiation incubation. Error bars indicate SD of the mean for $N = 6$ independent experiments.

after irradiation of the MG-63 cells, in spite of the significant increases in both the CH_2 and CH_3 mobile lipids.

It is extremely interesting that the ^{1}H-NMR visible lipids correlate with the cell proliferation status [2, 37,40]. Rosi *et al.* reported the increased CH_2/CH_3 lipid signal intensity ratio for the HeLa cells treated with the antitumor drug lonidamine, which blocks cell proliferation and cell progression through the cycle [40]. The effect was visible 24 h after the treatment ($CH_2/CH_3 = 1.91 \pm 0.2$) and was increasing up to 48 h ($CH_2/CH_3 = 4.1 \pm 0.4$). After 72 h the value was still close to the previous level ($CH_2/CH_3 = 4.3 \pm 0.4$). They suggested that when the cell cycle progression is blocked, triglyceride concentration remains high and the lipids accumulate in cells. As our results reveal, despite the high percentage of the G1-phase, the intensity of the CH_2 lipid signals is high in the ^{1}H NMR spectra of irradiated C6 cells.

Quintero *et al.* showed a possible cellular explanation of the NMR-visible mobile lipid changes in the growing C6 cells [37]. They suggest that in the normal growing conditions the lipid droplets associated with cytoskeleton are too small and their mobility is too low for being NMR visible. On proliferation arrest the phospholipids resynthesis is halted, and the small triacylglycerides containing bodies are transported through the cellular membranes for the phospholipids resynthesis which allows the accumulation and fusion of

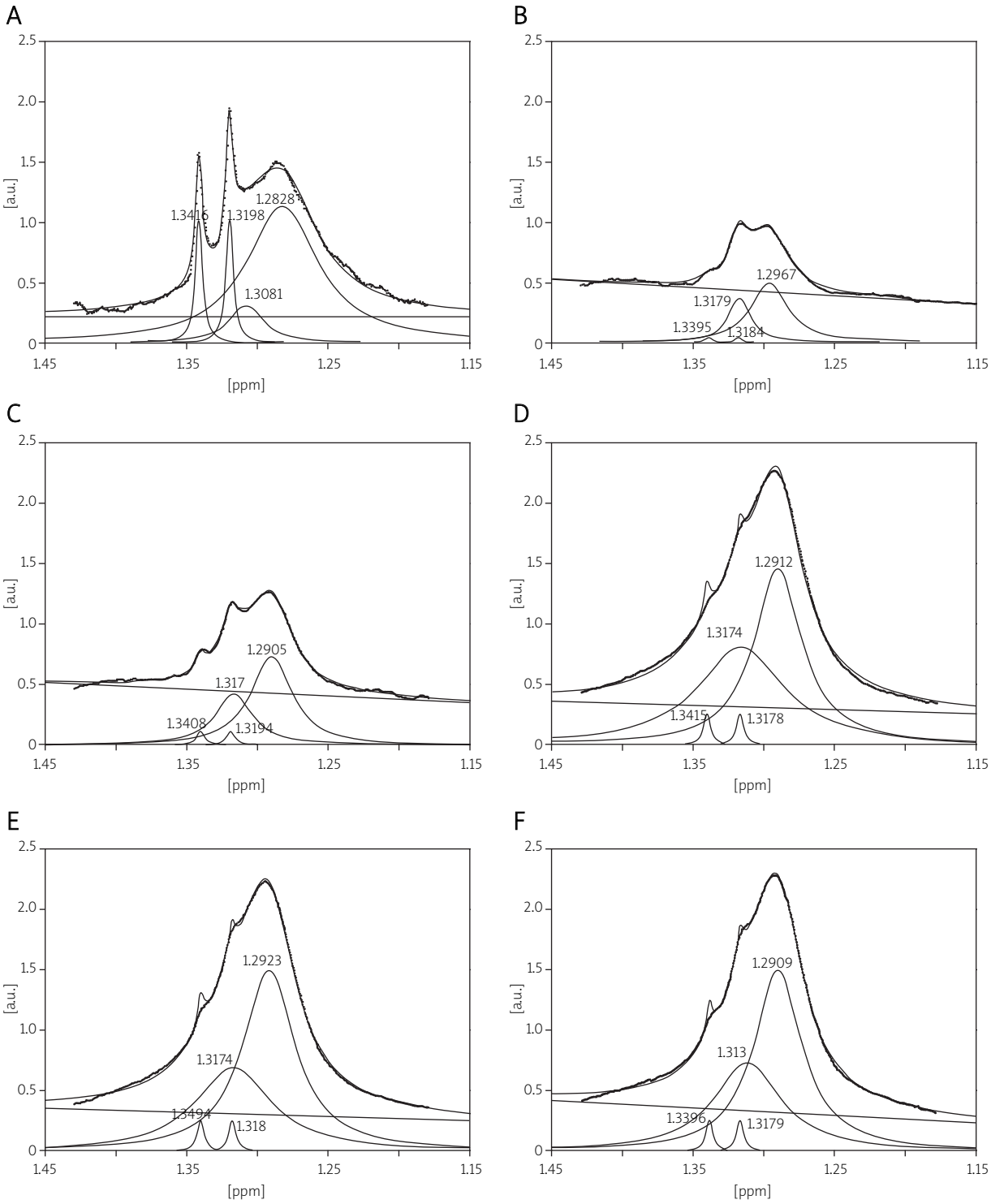

Fig. 6. Methylene lipid range (1.18-1.43 ppm) with Lorentz functions fitting according to Hiltunen *et al.* methodology [18] for **A**) dead cells, **B**) non-irradiated cells, **C**) irradiated cells and incubated for 24 h, **D**) irradiated cells and incubated for 48 h, **E**) irradiated cells and incubated for 72 h, **F**) irradiated cells and incubated for 96 h. Values over peaks represent central positions of individual resonance lines given in ppm.

the lipid bodies. When the size of the fusing droplets exceeds certain value (around 100 nm) and the mobility is high enough, the lipid content becomes NMR visible.

In our experiment, the proliferation arrest in the cells studied 24 h after irradiation (the decrease in G2/M + S) is small as compared to the non-irradiated cells at the same time point of incubation (as the flow cytometric measurements reveal). At longer incubation times both the irradiated cells and non-irradiated ones still reveal the decreased proliferation rates with no statistical differences between the cell percentages in the G1, G2/M and S phases (see Fig. 2). However, the CH_2/CH_3 lipid resonance ratio increase is observed exclusively for the irradiated cells. Therefore, the explanation postulated by Quintero *et al.* cannot be fully confirmed [37]. As they suggest, the amount of the NMR detectable mobile lipids in the viable C6 tumour cells should correlate with the proliferation rate changes of these cells.

Rainaldi *et al.* [38] report the variations in the ^{1}H-NMR metabolites in the HL60 cells due to apoptosis induced by ionizing radiation or the doxorubicin administration and due to necrosis induced by heating. Interestingly, in their experiment the lactate concentration in the cells irradiated with gamma-rays (the dose of 100 Gy) is found to increase in over 80%, whereas in the heated necrotic cells the lactate concentration increase is much higher (180%). In our experiment the lactate resonances do not vary significantly after the irradiation and incubation in both the irradiated and non-irradiated cells (as measured as the percentage area of the doublet peak at 1.33 ppm within the methylene lipid range). Thus, it may be concluded that the variations in the methylene lipids range after irradiation of the cells are caused mainly by fatty acyl chains of triglycerides inside cytosolic lipid droplets, while the contribution of lactate is small.

Conclusion

A significant increase in the CH_2 resonance peak was observed in the C6 cells exposed to 3.8 Gy after 24-96 h incubation while the CH_3 resonance peak remained unchanged.

The analysis of the cell cycle by a flow cytometry did not reveal evident apoptosis both in the irradiated cells and non-irradiated ones. In the case of the irradiated cells, no significant influence of irradiation on the proliferation arrest for the cells incubated at the times from the range of 48 h to 96 h was observed. Our data suggest that the increase in the CH_2/CH_3 lipid ratio in the irradiated C6 cells is not correlated with the cell death or the proliferation status and presumably is due to some modifications of the cell lipid composition after irradiation leading to the increased lipid mobility.

The described method of sample preparation enables the metabolic effects of irradiation to be observed in viable cells, which can effectively support identification of the spectroscopic changes *in vivo*. Application of the gel suspensions in the NMR studies has advantages over the usual liquid suspensions in terms of improved reproducibility of the data and cell viability, with no net loss of the spectral quality. Hereby it was shown, that *in vitro* ^{1}H NMR technique is useful in the non-invasive studies of the living cells response to irradiation and provides the essential information on dynamics of the metabolic processes after irradiation.

Acknowledgments

We wish to thank Zbigniew Maniakowski, MSc, for establishment of the irradiation procedure and dosimetry for the experiment. We also wish to thank Adam Bekman, MSc, Małgorzata Ganowicz, MSc, Bożena Woźniak, MSc, Łukasz Niewiadomski, MSc, and Marek Szewczuk, MSc, for their assistance with the irradiation procedures.

Supported by grant No. KBN 2P05E06829.

References

1. Al-Saffar NMS, Titley JC, Robertson D, Clarke PA, Jackson LE, Leach MO, Ronen SM. Apoptosis is associated with triacylglycerol accumulation in Jurkat T-cells. Br J Cancer 2002; 86: 963-970.
2. Barba I, Cabanas ME, Arus C. The relationship between nuclear magnetic resonance-visible lipids, lipid droplets, and cell proliferation in cultured C6 cells. Cancer Res 1999; 59: 1861-1868.
3. Barba I, Mann P, Cabanas ME, Arus C, Gasparovic C. Mobile lipid production after confluence and pH stress in perfused C6 cells. NMR Biomed 2001; 14: 33-40.
4. Benderitter M, Vincent-Genod L, Pouget JP, Voisin P. The cell membrane as a biosensor of oxidative stress induced by radiation exposure: a multiparameter investigation. Radiat Res 2003; 159: 471-483.
5. Bezabeh T, Mowat MR, Jarolim L, Greenberg AH, Smith IC. Detection of drug-induced apoptosis and necrosis in human cervical carcinoma cells using 1H NMR spectroscopy. Cell Death Differ 2001; 8: 219-224.
6. Blankenberg FG, Katsikis PD, Storrs RW, Beaulieu C, Spielman D, Chen JY, Naumovski L, Tait JF. Quantitative analysis of apopto-

tic cell death using proton nuclear magnetic resonance spectroscopy. Blood 1997; 89: 3778-3786.
7. Bouzier AK, Goodwin R, de Gannes FM, Valeins H, Voisin P, Canioni P, Merle M. Compartmentation of lactate and glucose metabolism in C6 glioma cells. A 13c and 1H NMR study. J Biol Chem 1998; 273: 27162-27169.
8. Bouzier AK, Voisin P, Goodwin R, Canioni P, Merle M. Glucose and lactate metabolism in C6 glioma cells: evidence for the preferential utilization of lactate for cell oxidative metabolism. Dev Neurosci 1998; 20: 331-338.
9. Callies R, Sri-Pathmanathan RM, Ferguson DY, Brindle KM. The appearance of neutral lipid signals in the 1H NMR spectra of a myeloma cell line correlates with the induced formation of cytoplasmic lipid droplets. Magn Reson Med 1993; 29: 546-550.
10. Day SE, Kettunen MI, Cherukuri MK, Mitchell JB, Lizak MJ, Morris HD, Matsumoto S, Koretsky AP, Brindle KM. Detecting response of rat C6 glioma tumors to radiotherapy using hyperpolarized [1-13C]pyruvate and 13C magnetic resonance spectroscopic imaging. Magn Reson Med 2011; 65: 557-563.
11. Delikatny EJ, Cooper WA, Brammah S, Sathasivam N, Rideout DC. Nuclear magnetic resonance-visible lipids induced by cationic lipophilic chemotherapeutic agents are accompanied by increased lipid droplet formation and damaged mitochondria. Cancer Res 2002; 62: 1394-1400.
12. Di Vito M, Lenti L, Knijn A, Iorio E, D'Agostino F, Molinari A, Calcabrini A, Stringaro A, Meschini S, Arancia G, Bozzi A, Strom R, Podo F. 1H NMR-visible mobile lipid domains correlate with cytoplasmic lipid bodies in apoptotic T-lymphoblastoid cells. Biochim Biophys Acta 2001; 1530: 47-66.
13. Grande S, Giovannini C, Guidoni L, Luciani AM, Palma A, Rosi A, Sapora O, Viti V. 1H MRS signals from glutathione may act as predictive markers of apoptosis in irradiated tumour cells. Radiat Prot Dosimetry 2006; 122: 205-206.
14. Grande S, Luciani AM, Rosi A, Palma A, Giovannini C, Sapora O, Guidoni L, Viti V. Metabolism of glutathione in tumour cells as evidenced by 1H MRS. FEBS Lett 2007; 581: 637-643.
15. Hakumaki JM, Brindle KM. Techniques: Visualizing apoptosis using nuclear magnetic resonance. Trends Pharmacol Sci 2003; 24: 146-149.
16. Hakumaki JM, Kauppinen RA. 1H NMR visible lipids in the life and death of cells. Trends Biochem Sci 2000; 25: 357-362.
17. Hakumaki JM, Poptani H, Sandmair AM, Yla-Herttuala S, Kauppinen RA. 1H MRS detects polyunsaturated fatty acid accumulation during gene therapy of glioma: implications for the in vivo detection of apoptosis. Nat Med 1999; 5: 1323-1327.
18. Hiltunen Y, Ala-Korpela M, Jokisaari J, Eskelinen S, Kiviniitty K, Savolainen M, Kesäniemi YA. A lineshape fitting model for 1H NMR spectra of human blood plasma. Magn Reson Med 1991; 21: 222-232.
19. Iliakis G, Wang Y, Guan J, Wang H. DNA damage checkpoint control in cells exposed to ionizing radiation. Oncogene 2003; 22: 5834-5847.
20. Iorio E, Di Vito M, Spadaro F, Ramoni C, Lococo E, Carnevale R, Lenti L, Strom R, Podo F. Triacsin C inhibits the formation of 1H NMR-visible mobile lipids and lipid bodies in HuT 78 apoptotic cells. Biochim Biophys Acta 2003; 1634: 1-14.
21. Kondo T, Setoguchi T, Taga T. Persistence of a small subpopulation of cancer stem-like cells in the C6 glioma cell line. Proc Natl Acad Sci U S A 2004; 101: 781-786.
22. Kuesel AC, Sutherland GR, Halliday W, Smith IC. 1H MRS of high grade astrocytomas: mobile lipid accumulation in necrotic tissue. NMR Biomed 1994; 7: 149-155.
23. Kurimoto M, Endo S, Hirashima Y, Hamada H, Ogiichi T, Takaku A. Growth inhibition and radiosensitization of cultured glioma cells by nitric oxide generating agents. J Neurooncol 1999; 42: 35-44.
24. Lehtimäki KK, Valonen PK, Griffin JL, Väisänen TH, Gröhn OH, Kettunen MI, Vepsäläinen J, Ylä-Herttuala S, Nicholson J, Kauppinen RA. Metabolite changes in BT4C rat gliomas undergoing ganciclovir-thymidine kinase gene therapy-induced programmed cell death as studied by 1H NMR spectroscopy in vivo, ex vivo, and in vitro. J Biol Chem 2003; 278: 45915-45923.
25. Li Y, Owusu A, Lehnert S. Treatment of intracranial rat glioma model with implant of radiosensitizer and biomodulator drug combined with external beam radiotherapy. Int J Radiat Oncol Biol Phys 2004; 58: 519-527.
26. Luciani AM, Grande S, Palma A, Rosi A, Giovannini C, Sapora O, Viti V, Guidoni L. Characterization of 1H NMR detectable mobile lipids in cells from human adenocarcinomas. FEBS J 2009; 276: 1333-1346.
27. Lundberg P, Roy S, Kuchel PW. Immobilization methods for NMR studies of cellular metabolism – a practical guide. Immunomethods 1994; 4: 163-178.
28. Mao XW, Green LM, Gridley DS. Evaluation of polysaccharopeptide effects against C6 glioma in combination with radiation. Oncology 2001; 61: 243-253.
29. Matulewicz L, Sokol M, Wydmanski J, Hawrylewicz L. Could lipid CH2/CH3 analysis by in vivo 1H MRS help in differentiation of tumor recurrence and post-radiation effects? Folia Neuropathol 2006; 44: 116-124.
30. Mikhailenko VM, Philchenkov AA, Zavelevich MP. Analysis of 1H NMR-detectable mobile lipid domains for assessment of apoptosis induced by inhibitors of DNA synthesis and replication. Cell Biol Int 2005; 29: 33-39.
31. Milkevitch M, Shim H, Pilatus U, Pickup S, Wehrle JP, Samid D, Poptani H, Glickson JD, Delikatny EJ. Increases in NMR-visible lipid and glycerophosphocholine during phenylbutyrate-induced apoptosis in human prostate cancer cells. Biochim Biophys Acta 2005; 1734: 1-12.
32. Murphy PS, Rowland IJ, Viviers L, Brada M, Leach MO, Dzik-Jurasz AS. Could assessment of glioma methylene lipid resonance by in vivo (1)H-MRS be of clinical value? Br J Radiol 2003; 76: 459-463.
33. Ormerod MG, Kubbies M. Cell cycle analysis of asynchronous cell populations by flow cytometry using bromodeoxyuridine label and Hoechst-propidium iodide stain. Cytometry 1992; 13: 678-685.
34. Parthymou A, Kardamakis D, Pavlopoulos I, Papadimitriou E. Irradiated C6 glioma cells induce angiogenesis in vivo and activate endothelial cells in vitro. Int J Cancer 2004; 110: 807-814.
35. Pérez Y, Lahrech H, Cabańas ME, Barnadas R, Sabés M, Rémy C, Arús C. Measurement by nuclear magnetic resonance diffusion of the dimensions of the mobile lipid compartment in C6 cells. Cancer Res 2002; 62: 5672-5677.
36. Plate KH, Breier G, Millauer B, Ullrich A, Risau W. Up-regulation of vascular endothelial growth factor and its cognate receptors

in a rat glioma model of tumor angiogenesis. Cancer Res 1993; 53: 5822-5827.
37. Quintero M, Cabanas ME, Arus C. A possible cellular explanation for the NMR-visible mobile lipid (ML) changes in cultured C6 glioma cells with growth. Biochim Biophys Acta 2007; 1771: 31-44.
38. Rainaldi G, Romano R, Indovina P, Ferrante A, Motta A, Indovina PL, Santini MT. Metabolomics using 1H-NMR of apoptosis and Necrosis in HL60 leukemia cells: differences between the two types of cell death and independence from the stimulus of apoptosis used. Radiat Res 2008; 169: 170-180.
39. Riemann B, Könemann S, Pöpping D, Kopka K, Weckesser M, Willich N, Schober O. Early effects of irradiation on [(123)I]-IMT and [(18)F]-FDG uptake in rat C6 glioma cells. Strahlenther Onkol 2004; 180: 434-441.
40. Rosi A, Luciani AM, Matarrese P, Arancia G, Viti V, Guidoni L. 1H-MRS lipid signal modulation and morphological and ultrastructural changes related to tumor cell proliferation. Magn Reson Med 1999; 42: 248-257.
41. Santini MT, Ferrante A, Romano R, Rainaldi G, Motta A, Donelli G, Vecchia P, Indovina PL. A 700 MHz 1H-NMR study reveals apoptosis-like behavior in human K562 erythroleukemic cells exposed to a 50 Hz sinusoidal magnetic field. Int J Radiat Biol 2005; 81: 97-113.
42. Santini MT, Romano R, Rainaldi G, Ferrante A, Indovina P, Motta A, Indovina PL. 1H-NMR evidence for a different response to the same dose (2 Gy) of ionizing radiation of MG-63 human osteosarcoma cells and three-dimensional spheroids. Anticancer Res 2006; 26: 267-281.
43. Santini MT, Romano R, Rainaldi G, Ferrante A, Motta A, Indovina PL. Increases in 1H-NMR mobile lipids are not always associated with overt apoptosis: evidence from MG-63 human osteosarcoma three-dimensional spheroids exposed to a low dose (2 Gy) of ionizing radiation. Radiat Res 2006; 165: 131-141.
44. Santini MT, Romano R, Rainaldi G, Indovina P, Ferrante A, Motta A, Indovina PL. Temporal dynamics of 1H-NMR-visible metabolites during radiation-induced apoptosis in MG-63 human osteosarcoma spheroids. Radiat Res 2006; 166: 734-745.
45. Schmitz JE, Kettunen MI, Hu DE, Brindle KM. 1H MRS-visible lipids accumulate during apoptosis of lymphoma cells in vitro and in vivo. Magn Reson Med 2005; 54: 43-50.
46. Shih CM, Ko WC, Yang LY, Lin CJ, Wu JS, Lo TY, Wang SH, Chen CT. Detection of apoptosis and necrosis in normal human lung cells using 1H NMR spectroscopy. Ann N Y Acad Sci 2005; 1042: 488-496.
47. Suzuki K, Ojima M, Kodama S, Watanabe M. Radiation-induced DNA damage and delayed induced genomic instability. Oncogene 2003; 22: 6988-6993.
48. Thews O, Zywietz F, Lecher B, Vaupel P. Quantitative changes of metabolic and bioenergetic parameters in experimental tumors during fractionated irradiation. Int J Radiat Oncol Biol Phys 1999; 45: 1281-1288.
49. Watters D. Molecular mechanisms of ionizing radiation-induced apoptosis. Immunol Cell Biol 1999; 77: 263-271.
50. Zhang W, Yamada H, Sakai N, Nozawa Y. Sensitization of C6 glioma cells to radiation by staurosporine, a potent protein kinase C inhibitor. J Neurooncol 1993; 15: 1-7.
51. Zoula S, Herigault G, Ziegler A, Farion R, Decorps M, Remy C. Correlation between the occurrence of 1H-MRS lipid signal, necrosis and lipid droplets during C6 rat glioma development. NMR Biomed 2003; 16: 199-212.